Measurements in the wake of a ventilated hydrofoil: a step towards improved turbine aeration techniques

C Ellis[1], A Karn[1], J Hong[1], S-J Lee[2], E Kawakami[3], D Scott[4], J Gulliver[1], REA Arndt[1]

1 St. Anthony Falls Laboratory, University of Minnesota
2 Research Institute of Marine Systems Engineering, Seoul National University
3 3M Corporate Research Process Laboratory
4 ALSTOM Renewable Power Canada Inc.

Abstract The purpose of this study is to develop the necessary algorithms to determine the bubble size distribution and velocity in the wake of a ventilated or cavitating hydrofoil utilizing background illumination. A simplified experiment was carried out to validate the automatic bubble detection algorithm at the Saint Anthony Falls Laboratory (SAFL) of the University of Minnesota. The experiment was conducted in the SAFL high-speed water tunnel. First, particle shadow velocimetry (PSV) images of a bubbly flow were collected. Bubbles were identified in the images using an edge detection method based on the Canny algorithm. The utilized algorithm was designed to detect partly overlapping bubbles and reconstruct missing parts. After all images were analyzed, the bubble velocity was determined by applying a tracking algorithm. This study has shown that the algorithm enables reliable analysis of irregularly shaped bubbles even when bubbles are highly overlapped in the wake of the ventilated hydrofoil. It is expected that this technique can be used to determine the bubble velocity field as well as the bubble size distributions.

Introduction

The discharge by hydropower facilities of water that is low in dissolved oxygen is increasingly of concern due to its effect on downstream water quality. As a result, a number of techniques have been investigated that aerate the water employed, one being direct aeration by the hydroelectric turbine. To assess the efficacy of such strategies, coupled experimental and numerical approaches are needed that connect bubble size and behavior in high speed and highly turbulent flow to the physical processes governing gas transfer. The purpose of this study is to develop the necessary algorithms to determine the bubble size distribution and flow field in the wake of a ventilated hydrofoil utilizing background illumination. These data will provide an extensive and rich data set that can both be correlated to measurements of gas transfer efficiency and also used as a validation tool for computational studies of the two phase flow through ventilated hydroturbines.

For a detailed analysis of two-phase flows, non-intrusive optical techniques are most suitable. Such measurement techniques can provide the velocity fields and the local bubble size distributions. Phase-Doppler anemometry (PDA) has a higher sizing accuracy than direct imaging techniques when small spherical bubbles are studied, but accuracy decreases when the shape of the bubbles becomes non-spherical and their size increases. Laser light sheet illumination is very useful for large-scale measurements. However, a remaining problem for the application of particle image velocimetry (PIV) to bubbly flows is the strong absorption of the penetrating laser light sheet by scattering on the surface of the bubbles, particularly in dense bubble clouds. One technique that allows the quantifying of bubble size, shape, and distribution is shadow imaging using a diffuse back-light. A problem that arises in higher void fraction bubbly flows is that of highly overlapping bubble images which may include in-focus and out-of-focus bubbles. A reliable algorithm is necessary to reconstruct missing parts of overlapping bubbles. There is also the issue of image calibration and the determination of appropriate length scales. Unless a telecentric lens is used in the imaging system, the length scale

(real world length per pixel) increases with distance from the camera. A rationale needs to be established that assigns appropriate lengths to the acquired images. This affects both the estimation of bubble size and bubble velocity.

The objective of the present study is to develop the necessary algorithms to determine the bubble size distribution and velocity field in the wake of a ventilated hydrofoil using background illumination. Velocity fields were derived using particle tracking techniques applied to the shadow images The in-focus bubbles, those in the camera's depth of field, cast the darkest, most distinct shadows. Image depth-of-field is determined by the camera setup and can be used to determine the location and thickness of the measurement plane. This is important in establishing the needed length scales in the images. Using shadow images, the size, number, distribution, and velocity of bubbles in the wake of a ventilate hydrofoil were determined.

Experimental Set Up

The experiments were conducted in the high-speed water tunnel at Saint Anthony Falls Laboratory (SAFL) of the University of Minnesota. The tunnel is capable of velocities in excess of 20 *m/s*. The test section measures 0.19*m* (W) x 0.19*m* (H) x 1.2*m* (L), and is fitted with observation windows on three sides. A special design of the tunnel allows for the removal of large quantities of air during experiments, allowing for long time-period experiments with little to no effect on test section conditions. Figure 1 provides a schematic of the SAFL water tunnel. A NACA0015 hydrofoil was installed in the test section employing a cylindrical mounting plug that allowed easily adjustable angles of attack (α). The hydrofoil is 190 *mm* in span and 81 *mm* in chord. Air was injected into a slot spanning the hydrofoil by means of a compressed air line. This air injection slot had a width of 0.5 *mm* and was located 5 *mm* from the leading edge. A special design of internal ducting insured an even air distribution across the span of the hydrofoil.

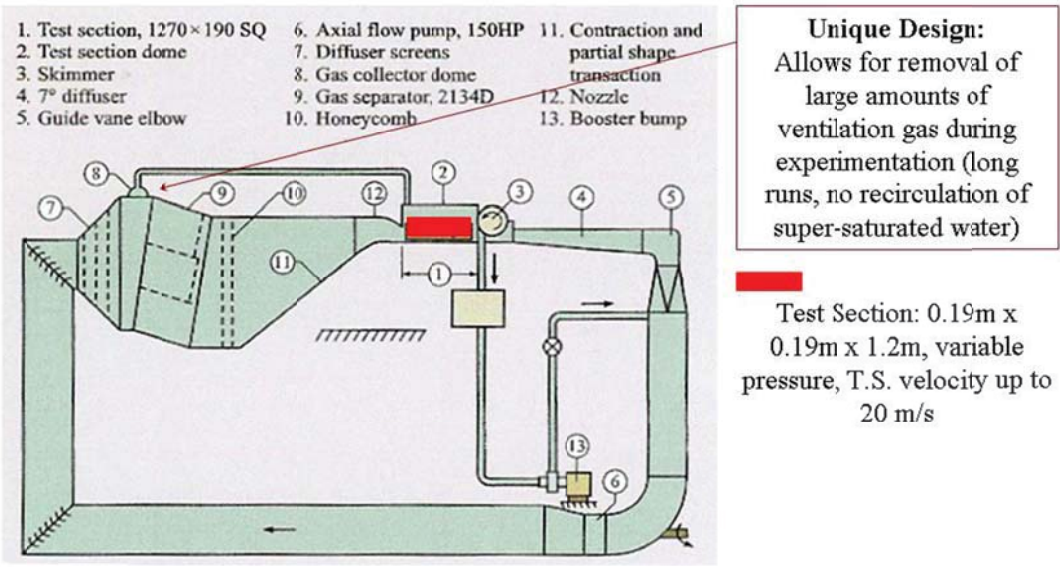

Figure 1. SAFL water tunnel

Figure 2 is a schematic of the optical experimental setup. A custom-made pulsed LED light source from ISSI was used to illuminate the flow. The pulsed LED array is capable of flash rates up to 10 *k*Hz with a minimum 5 microsecond pulse width (flash duration) and rise and fall times ~200

nanoseconds. Equipped with TTL control, the light source could easily be integrated with a LaVision TR-PIV system. This allowed the light source to be used for the acquisition of periodic image pairs (known as frame straddling) used by the in-house developed bubble tracking algorithm to calculate randomly located velocity vector fields and associated statistics or for high speed time series image acquisition needed to produce time resolved velocity fields such as is used in the tracking of coherent structures. To improve the uniformity of back-lighting in the images, a light shaping diffuser was placed between the light source and the test section. This improved the image processing associated with both the bubble size analysis and PSV. A 1-megapixel Photron APX-RS camera, capable of 3000 frames per second at full resolution (up to 250,000 fps at limited resolution) was used to obtain images.

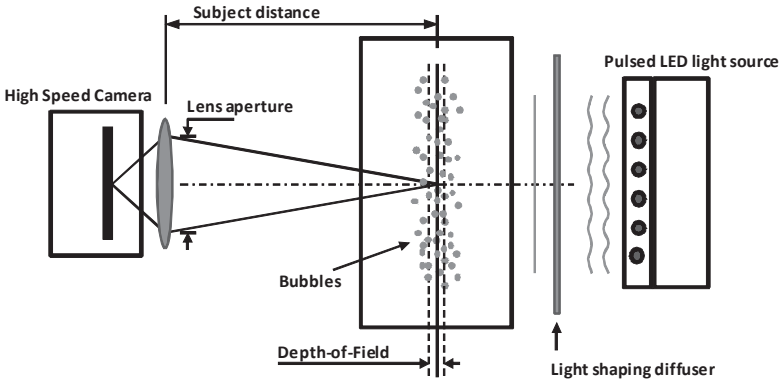

Figure 2. Schematic of optical experimental setup

In our initial studies, a 60 *mm* lens was used. The depth-of-field was 0.87 *mm* with the f-number of 2.8 modified by a spacer of 46.5 *mm* in width. The time between frame-straddled LED pulses (dt) was 50 μs. During these experiments, the incoming flow velocity was maintained at 7.0 *m/s*. The flow rate of injected air passing though the hydrofoil was 0.094 m^3/Hr, and the pulse width of the LED array was 15 μs.

Initial Studies

Image Processing-Overlapping bubbles in bubble shadow images need to be identified and individual bubbles reconstructed to accurately assess bubble size, shape, distribution, and (using particle tracking methods) velocity. Hence a robust, reliable algorithm is required to separate bubble clusters into individual bubbles. Figure 3 provides an overview of the image processing procedure for distinguishing individual bubbles from a cluster of overlapping bubbles. First, the background can be removed by subtracting a reference image taken for the same setup without bubbles. Then, all parts of the image are segmented on the basis of a Canny edge detector (Canny, 1986). To distinguish individual bubbles from the group of overlapping bubble images, several algorithms have been developed to reconstruct missing parts of partially obscured bubbles. A curvature profile based method (refer to Honkanen et al., 2005; Pla, F., 1996) was applied in this work. The curvature along the perimeter represents the shape change of the perimeter. Several negative peaks of the curvature indicate potential connecting points which divide the perimeter into parts. For processing, peaks can be chosen arbitrarily and an ellipse is fitted to a partial perimeter by selecting two connecting points using a non-linear least squares method provided in Matlab. If the overlapping ratio S_o/S_e, i.e. the ratio

of the area of a partial perimeter (S_o) to the area of a fitted ellipse (S_e), satisfies a threshold criterion, the fitted ellipse is determined to be a bubble. The maximum overlapping ratio was set to 50% in this study. To avoid highly flattened ellipses (i.e. an ellipse with high eccentricity) and smaller ellipses that either are noise or errors from a partial perimeter, the radii of an ellipse are constrained by upper and lower limits depending on the size of the bubble of interest. This procedure is then repeated and individual bubbles are successfully recognized from a cluster of bubbles as shown in figure 3.

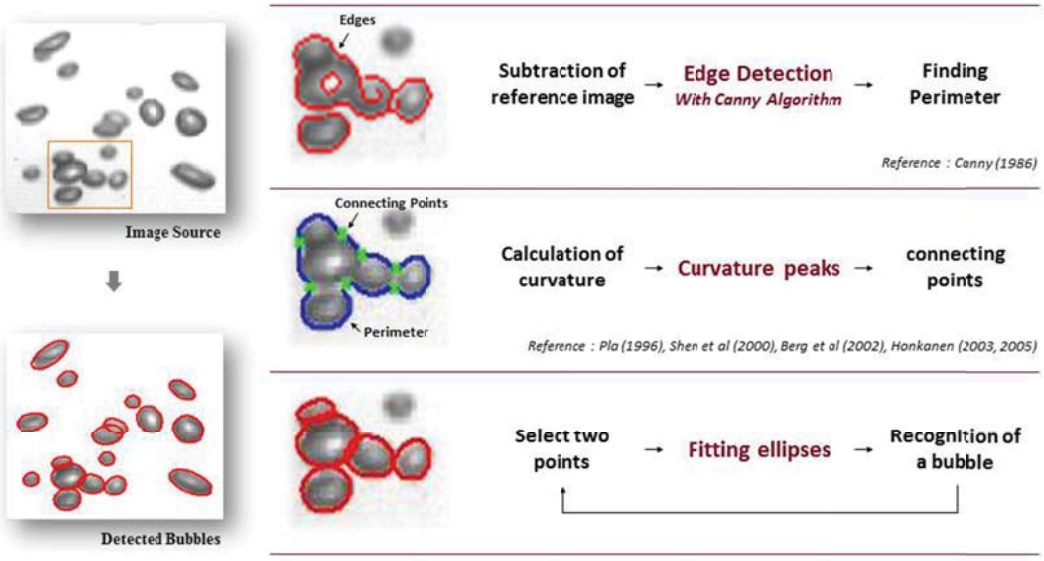

Figure 3. Consecutive steps illustrating bubble processing of the representative shadow image shown in top left*:* The edges are first segmented by a Canny edge detector. Then the curvature of the perimeters is determined to identify connecting points, where individual elliptical shaped bubbles can be fitted.

Initial Results-Our optical concept was first tested at relatively low air injection rates. Shadow images of a bubbly flow were collected as shown in figure 4. To have minimum inclusion of out-of-focus bubbles in the region of interest, image intensities were adjusted before applying the proposed bubble detection algorithm. 100 image pairs were analyzed by the bubble detection algorithm and roughly 230 randomly located velocity vectors per image pair were calculated using a bubble identification and tracking algorithm.

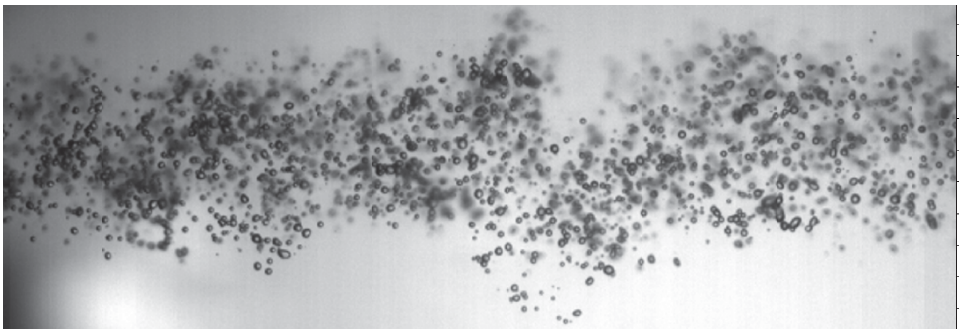

Figure 4. Bubble shadow image from back light illumination

The histograms of the area-equivalent radius and eccentricity (defined as ratio of major to minor diameter of an ellipse, b/a) of the detected bubbles are shown in Figure 5. Using this definition, the eccentricity of a circle is 1, and the eccentricity of an ellipse is greater than zero but less than 1. Most of the detected bubbles have eccentricities close to 1 with a radius of 0.2 - 0.3 *mm*. Figure 6 shows the distribution of area-equivalent bubble radius ($=\sqrt{ab}$) in the wake of the ventilated hydrofoil. As the figure shows, the bubble radius increases slightly downstream in the wake. The average radius increase is roughly 4% across the domain shown.

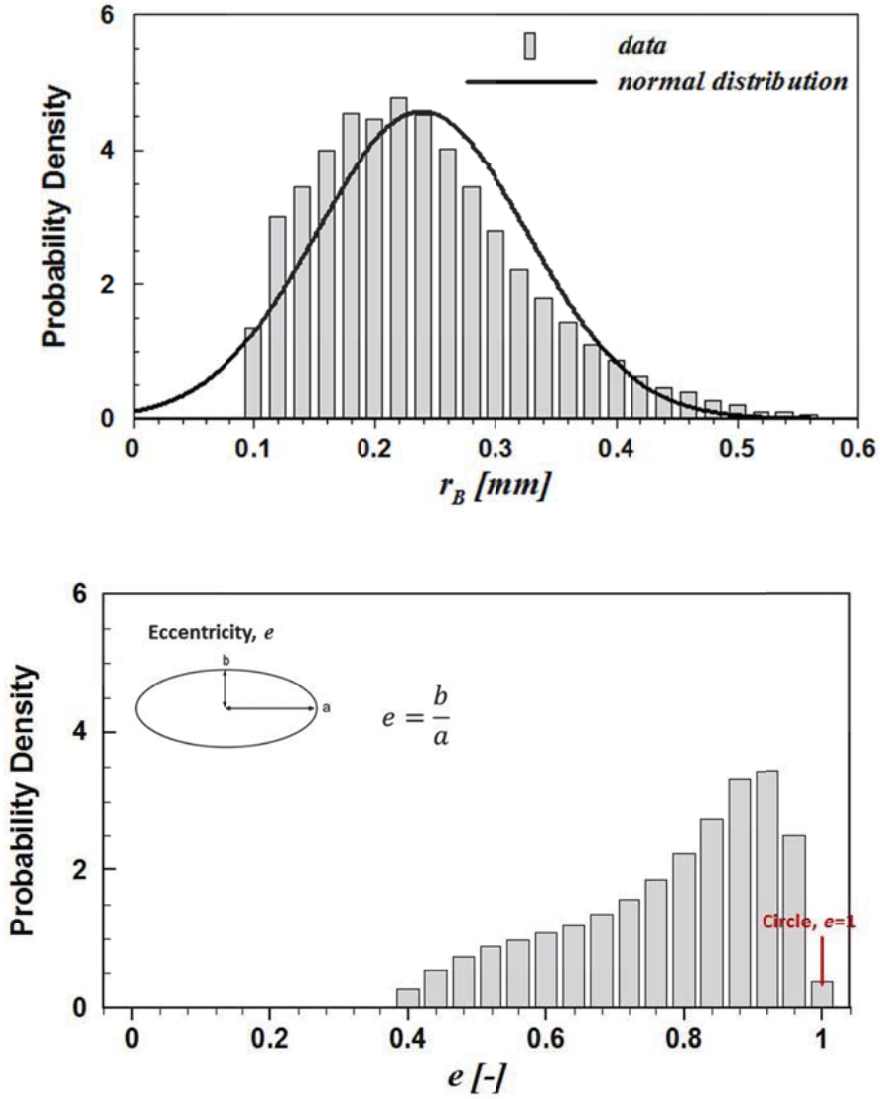

Figure 5. Histograms of the area-equivalent radius *(top)* and eccentricity of bubbles *(bottom)*. Adapted from Lee et al (2013)

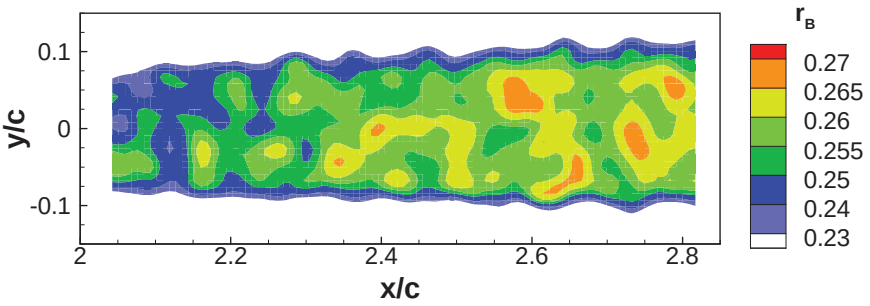

Figure 6. Area-equivalent bubble radius

The bubble velocity was calculated by the displacement of the bubble centroid. The randomly located velocity vectors were interpolated onto a uniform rectangular grid, and the whole field was smoothed to account for regions without sufficient bubbles. The bubble velocities were normalized by the free stream velocity of 7 *m/s*. Figure 7 shows the averaged normalized streamwise velocity in the wake behind the hydrofoil. The spatially averaged values of normalized streamwise and vertical velocities are 0.91 and 0.02, respectively. The low velocity band near the boundary of the contoured bubble field results from Gaussian interpolation since the velocity field cannot be measured outside the wake where no bubbles are present. Keeping in mind that a very small number of data pairs were analyzed, the measured bubble velocity distribution appears to represent the velocity field of the wake behind the ventilated hydrofoil.

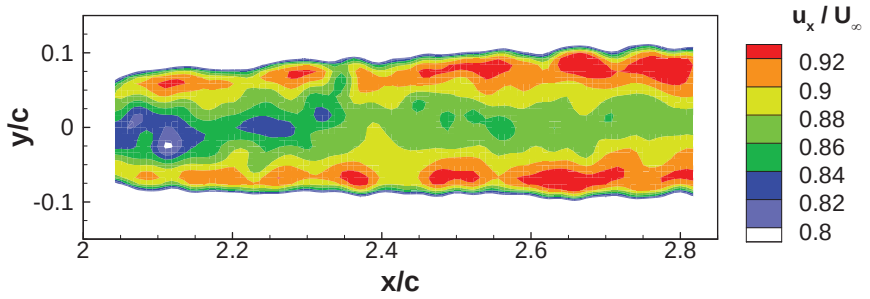

Figure 7. Streamwise velocity contour

Figure 8 shows normalized velocity deficit profiles of bubbles in the two-phase flows of this study and those associated with a pure liquid (single-phase flow). The pure liquid velocity field was measured by conventional PIV with dual head Nd:YAG lasers and optics. The velocity deficits are recovered downstream with similar trends between bubbles and pure liquid. There are differences in the velocity deficit between the bubble and liquid phase in the center of the wake, and the results imply that the spreading of the wake in a ventilating flow is significantly larger than that of the non-ventilated, single-phase flow.

Extension to Higher Airflow Rates-Our initial bubble analysis was carried out at relatively low airflow rates. It was found that as airflow rate was increased, bubble fields were produced that were much too dense to employ the bubble shadow technique in its original configuration. This is illustrated in Figure 9. As shown in the figure, bubbles became indistinguishable at the higher flow rates that were deemed necessary for a practical air injection system. Lacking a viable alternative

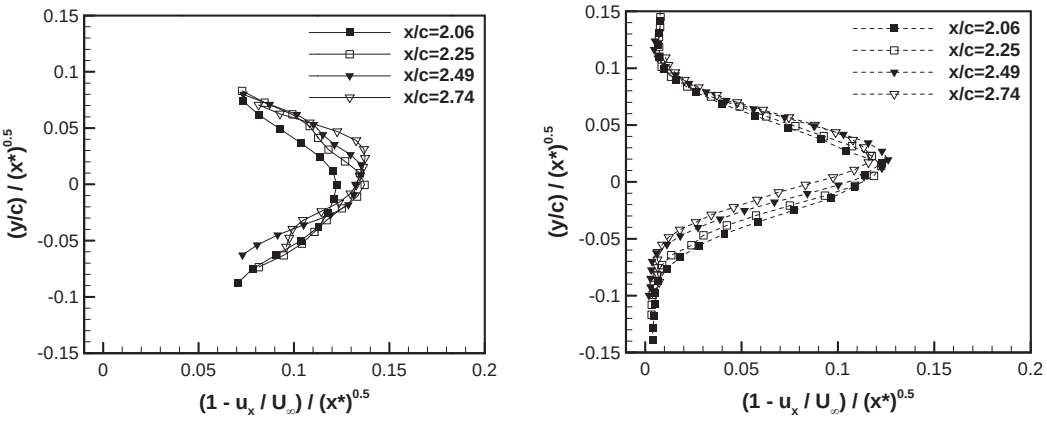

Figure 8. Vertical profiles of averaged streamwise velocity of bubbles in the two-phase flow (left) and a liquid in the single-phase flow (right) (Data are scaled in similarity variables for turbulent plane wakes (refer to Fig. 15.63 in Tropea et al. (2007)). Coordinate x is the distance from the trailing edge.

measurement technique, it was decided to reduce the ventilation slot length by 95%, masking off all but the center 5% of the slot. The air flow rates used in the gas transfer experiments were likewise reduced by 95% for these tests maintaining the specific air discharge (flow rate per unit slot length). All other parameters were held constant. It was felt that this technique would be equivalent to illuminating the wake with a thin sheet of light. The 5% unmasked slot length was sufficiently small to allow nearly all of the bubbles to be in focus (i.e. within the depth of field) allowing the possibility of performing a mass balance between the total amount of air injected and the total amount of air associated with the measured bubbles. The limitations to this experimental simplification are recognized, but after careful consideration, it was felt that the methodology was justified particularly lacking any viable measurement alternative.

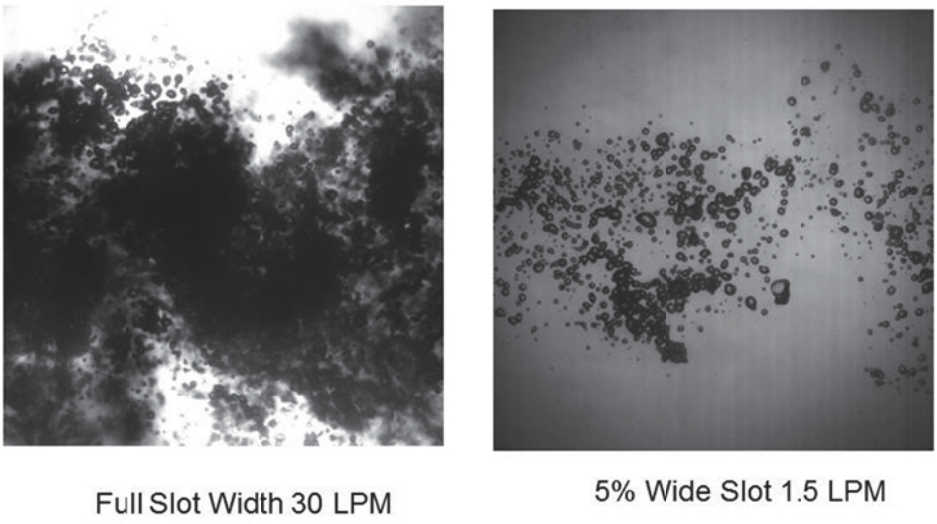

Figure 9. Comparison of bubbly wake with full slot ventilation and with all but center 5% of slot length masked.

An additional problem was that the previously developed approach for extracting the bubble size information from the captured digital images was computationally expensive (approx. 20 minutes per image). Also, the algorithm failed to resolve large clusters and was also limited in detecting bubbles which were slightly out-of-focus. Out-of-focus or small bubbles were eliminated in a pre-processing step under this scheme. To overcome these limitations, a robust and integrated image analysis based on multi-level segmentation was developed for a bubbly flow with a wide bubble size distribution in the size range of 170 microns to 1.5 mm. The bubble detection is carried out at multiple levels. First, in-focus and out-of-focus bubbles are separated. Next, within these two groups, a customized morphological technique and watershed segmentation (Meyer 1994) are employed respectively to resolve the overlapped clusters. Thus, all the relevant information from bubble images was extracted to the maximum extent possible. This procedure is illustrated schematically in figure 10. Additionally, the newly developed image-processing algorithm reduced the processing time to less than 10 seconds per image. The image processing was then parallelized over 8 cores to further reduce the required processing time to about a second per image. This enabled the analysis of 1000 bubble images for each test condition in about 20 minutes. A total of 45,000 frame straddled image pairs were acquired as part of this phase of the test program.

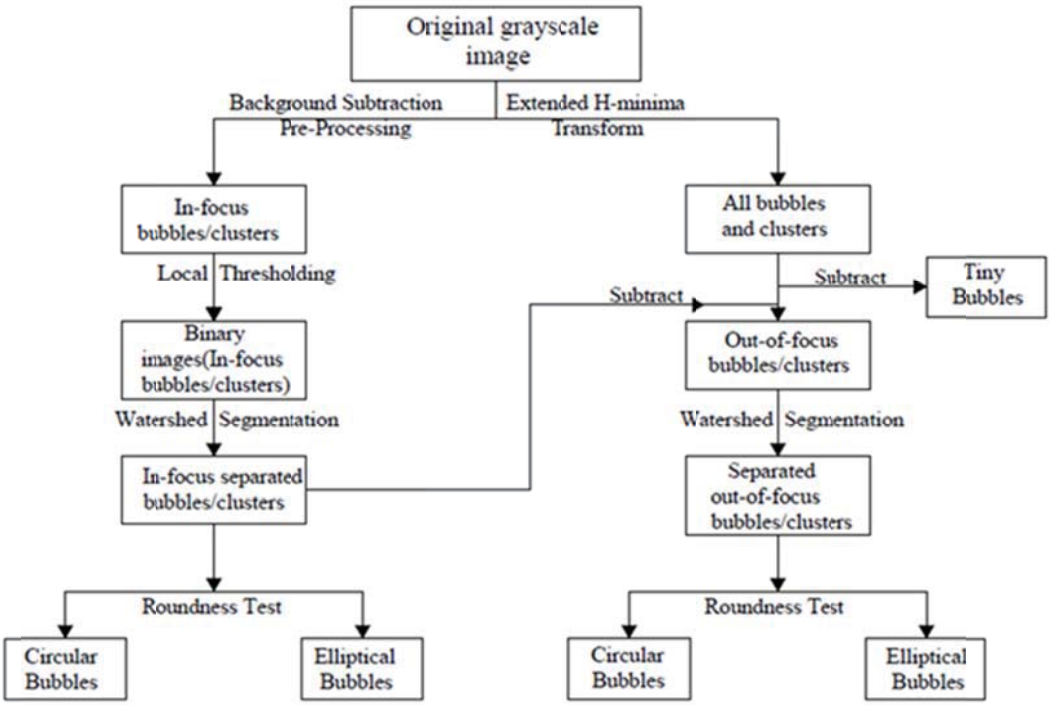

Figure 10 Schematic of new image processing technique

The original technique for acquiring bubble images was also improved. A calibration grid was fabricated, inserted at the water tunnel centerline, and used to calibrate the images and determine image length scale (pixel size). This is needed for both the assessment of bubble size and shape and for the determination of the bubble velocity. The camera's depth of field was adjusted such that nearly all of the bubbles visualized were in focus. Of course, not all of the bubbles visualized were precisely at the test section centerline. The unmasked slot length (9.6mm) spanned a distance +/- 4.8mm around the camera's focus distance of 299mm. This results in a length scale uncertainty of

+/- 1.6%. It was observed that the bubble field spread in width as it propagated through the wake by as much as a factor of 2 making the maximum associated length scale uncertainty +/- 3.2%.

Data were taken and analyzed for 15 test conditions at 3 locations downstream of the ventilated foil. For each test, images were acquired in the foil wake centered at 109mm, 243mm and 377mm (1.3C, 3C and 4.7C where C is the cord length of 81mm) downstream of the foil's center of rotation. For each test condition and position, the data consisted of 1000 frame-straddled image pairs taken over a 40 second period. Each image spanned a 60mm x 60mm square field of view resulting in an image resolution (pixel size) of 0.059mm. The flash delay associated with an image pair was optimized, based on free stream velocity, to provide approximately 20 pixel translations between images and varied from 120 to 230 microseconds. The flash duration was set to 15 microseconds for all images, sufficient to produce minimal blur under all test conditions. A sample result of the improved image analysis algorithm is shown in Figure 11. A typical bubble size distribution is shown in Figure 12. A comparison of figure 12 with figure 5 indicates that the results are similar to those obtained previously. This supports our assumption that masking off all but the center 5% of the slot accurately characterizes the flow physics for these experiments.

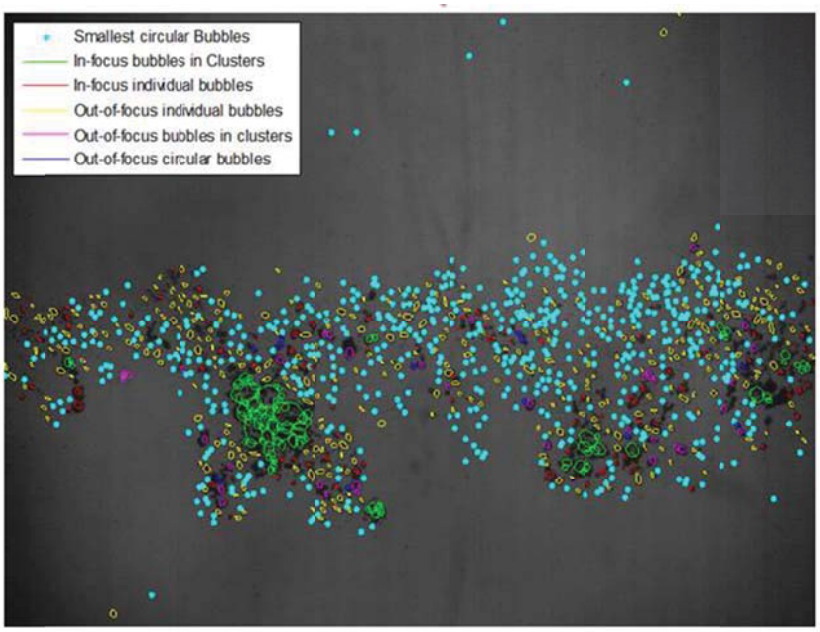

Figure 11. Preliminary calculations based on the current analysis gave a predicted volume flow rate of 0.47 – 0.49 LPM which compares favorably with the 0.5 LPM injected

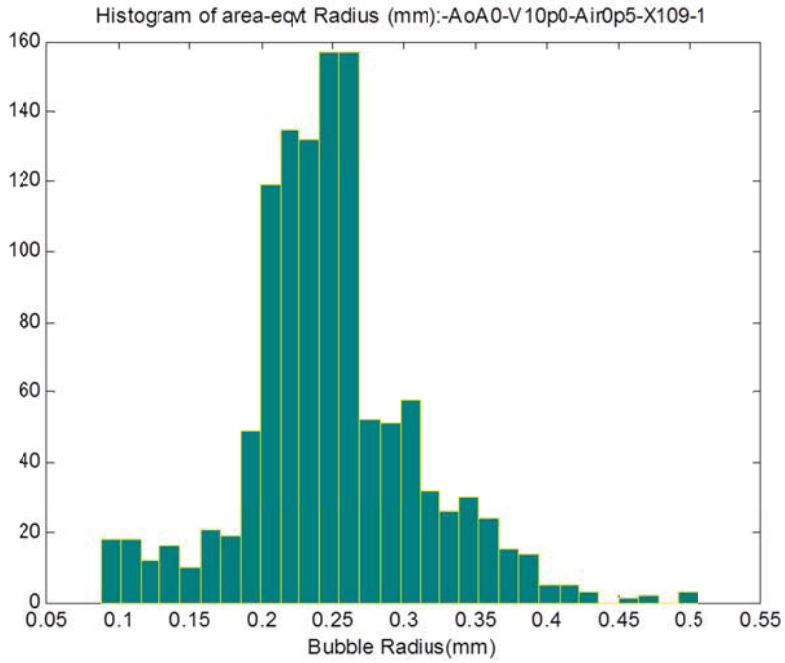

Figure 12. Typical bubble size distribution found with the new method.

Conclusion

A high speed bubble field image acquisition technique coupled to newly developed and improved algorithms to identify and characterize the bubble fields in the images were successfully implemented. Masking off all but the center 5% of the ventilation slot did not substantially alter the bubble size distribution, supporting our contention that the experiments accurately represent the flow physics of the original full slot gas transfer experiments. The wake behind a ventilated hydrofoil was investigated using the described techniques and algorithms. The bubbles in the wake of the ventilated hydrofoil were well captured, and, based on initial studies with only 100 image pairs, their velocities were seen to represent the velocity field of the wake. The velocity characteristics of a bubbly flow can be obtained with the shadow image technique described here including direct image processing methods. With further analysis, it is expected that this technique can be used to more fully characterize the associated bubble plume distribution and velocity field under a variety of test conditions.

Acknowledgments

Professor Can Kang (on leave from Jiangsu University) provided considerable help in interpreting the data. Special mention must go Dr. Seung-Jae Lee and Mr. Ellison Kawakami who are responsible for development of SIV technique and the initial bubble image processing have left the project, but have continued to provide input to the preparation of this paper.. This project is supported by grants from the DOE EERE – Wind & Water Power Program, Dr. Jose Zayas, Program Manager and ONR, Dr. Ron Joslin, Program Manager.

References

[1] Canny, J., A Computational Approach to Edge Detection, IEEE Transactions on PAMI, 8(6) , 679-698, (1986)
[2] Honkanen M., Saarenrinne, P., Stoor, T., Niinimaki, J. (2005), "Recognition of highly overlapping ellipse-like bubble images," *Measurement Science and Technology*, 16, 1760-1770.
[3] Pla, F., Recognition of Partial Circular Shapes from Segmented, Computer Vision and Image Understanding, 63(3), 334-343, (1996
[4] Lee,S-J. Kawakami, E. and Arndt, R.E.A. "Application of a shadow image velocimetry to a ventilated hydrofoil wake" Submitted to Journal of Visualization (2014)
[5] Tropea, C., Yarin, A.L. and Foss, J.F. (Eds), Handbook of Experimental Fluid Mechanics, Springer, (2007)
[6] Meyer, F., 'Topographic distance and watershed lines', Signal Processing, 38(1), pp.113-125, (1994)